

# Epidermis-on-a-chip system to develop skin barrier and melanin mimicking model

Journal of Tissue Engineering  
Volume 14: 1–13  
© The Author(s) 2023  
Article reuse guidelines:  
sagepub.com/journals-permissions  
DOI: 10.1177/20417314231168529  
journals.sagepub.com/home/tej



Qiwei Li<sup>1\*</sup>, Chunyan Wang<sup>1,2\*</sup>, Xiaoran Li<sup>1,3,4\*</sup>, Jing Zhang<sup>1,3,4</sup>,  
Zilin Zhang<sup>4</sup>, Keyu Yang<sup>4</sup>, Jun Ouyang<sup>4</sup>, Shaohui Zha<sup>4</sup>, Lifeng Sha<sup>4</sup>,  
Jianjun Ge<sup>3,4</sup>, Zaozao Chen<sup>1,3</sup>  and Zhongze Gu<sup>1,3</sup>

## Abstract

In vitro skin models are rapidly developing and have been widely used in various fields as an alternative to traditional animal experiments. However, most traditional static skin models are constructed on Transwell plates without a dynamic three-dimensional (3D) culture microenvironment. Compared with native human and animal skin, such in vitro skin models are not completely biomimetic, especially regarding their thickness and permeability. Therefore, there is an urgent need to develop an automated biomimetic human microphysiological system (MPS), which can be used to construct in vitro skin models and improve bionic performance. In this work, we describe the development of a triple-well microfluidic-based epidermis-on-a-chip (EoC) system, possessing epidermis barrier and melanin-mimicking functions, as well as being semi-solid specimen friendly. The special design of our EoC system allows pasty and semi-solid substances to be effectively utilized in testing, as well as allowing for long-term culturing and imaging. The epidermis in this EoC system is well-differentiated, including basal, spinous, granular, and cornified layers with appropriate epidermis marker (e.g. keratin-10, keratin-14, involucrin, loricrin, and filaggrin) expression levels in corresponding layers. We further demonstrate that this organotypic chip can prevent permeation of over 99.83% of cascade blue (a 607 Da fluorescent molecule), and prednisone acetate (PA) was applied to test percutaneous penetration in the EoC. Finally, we tested the whitening effect of a cosmetic on the proposed EoC, thus demonstrating its efficacy. In summary, we developed a biomimetic EoC system for epidermis recreation, which could potentially serve as a useful tool for skin irritation, permeability, cosmetic evaluation, and drug safety tests.

## Keywords

Epidermis-on-a-chip, barrier function, melanin, cosmetics, microfluidics

Date received: 28 November 2022; accepted: 22 March 2023

## Introduction

The skin is the largest organ in the body, forming a biological barrier to protect the body from foreign agents and pathogens. Though covered by a cornified layer, human skin can still be influenced and affected by a variety of conditions. Thus, it is important to detect and assess skin irritants, drug/pathogen penetration, as well as evaluating allergens, the aging effect of substances, and various skin disorders.<sup>1</sup> At present, pre-clinical research on new drugs and the optimization of cosmetics formulations relies on the application of various in vitro reproducible alternative models. However, animal models have limitations, due to ethical problems and high time and labor costs;

<sup>1</sup>State Key Laboratory of Bioelectronics, School of Biological Science and Medical Engineering, Southeast University, Nanjing, China

<sup>2</sup>State Key Laboratory of Space Medicine Fundamentals and Application, Chinese Astronaut Science Researching and Training Center, Beijing, China

<sup>3</sup>Institute of Medical Devices (Suzhou), Southeast University, Suzhou, China

<sup>4</sup>Jiangsu Avatarget Biotechnology Co., Ltd. Suzhou, China

\*These authors contributed equally to this work.

### Corresponding authors:

Zaozao Chen, State Key Laboratory of Bioelectronics, School of Biological Science and Medical Engineering, Southeast University, SiPaiLou #2, Nanjing 210096, China.  
Email: zaozaochen@seu.edu.cn

Zhongze Gu, State Key Laboratory of Bioelectronics, School of Biological Science and Medical Engineering, Southeast University, SiPaiLou #2, Nanjing 210096, China.  
Email: gu@seu.edu.cn



furthermore, there may be differences in thickness, hair density, and morphology among different animal models, resulting in poor predictability and repeatability of the obtained experimental results.<sup>2</sup> All of these factors have led to animal experimentation being prohibited for use in testing the toxicology of cosmetics in the EU since 2009 [(76/768/EEC, February 2003),<sup>3</sup> and the 3R principles—reduction, refinement, and replacement of animals in experiments—have been raised.<sup>4,5</sup> Cell- and Transwell-based skin models have become popular, and their complexity has been increasing. However, these models and their culture processes still lack the ability to fully mimic the skin micro-environment, which is a necessary condition for native human cell growth.<sup>6,7</sup>

As many publications have indicated, the “organ-on-a-chip (OOC)” is a recent developed technology which can reproduce sophisticated in vitro organ models, such as the skin.<sup>8,9</sup> This technology incorporates an automated, biomimetic, and microfluidic system for dynamic culture, using various in situ biosensors for non-invasive detection, which can help to expand their scope of application in the evaluation of drug candidates or cosmetics.<sup>5</sup> OOC technology may overcome clinical trial challenges by offering ways to conduct “clinical trials-on-chips” (CToCs) in ways not possible with other culture systems, leading to a next-generation trend in which OOC platforms bridge the gap between animal studies and clinical trials for the pharmaceutical industry.<sup>10</sup> Epidermis-on-a-chip technology has been reported for application in skin irritation<sup>11</sup> or drug efficacy<sup>12</sup> detection, as well as for the evaluation of side-effects of drugs.<sup>13</sup> EoCs can also be integrated with vascular structure, either by co-culturing with endothelial cells<sup>14</sup> or constructing pourable vascular channels.<sup>15</sup> Additionally, these micro-physiological systems also could perfuse or co-culture with immune cells<sup>16</sup>; this approach can help to investigate certain interactions relating to the immune system. Skin-connected interactions with other organs within integrated Organ-on-a-Chip systems have already been reported<sup>17,6</sup>; however, these works assessed barrier properties such as drug penetration using a skin surrogate—that is, a commercial membrane. In reality, a porous membrane (e.g. the widely used nitrocellulose filter membrane) is not an ideal biological skin equivalent. Therefore, an EoC for skin barrier mimicking is required.

Therefore, in this research, we describe the design of a triple-unit epidermis-on-a-chip that allows for three epidermises to be fabricated at the same time and allows for pasty and semi-solid substances tests. After air–liquid interface (ALI) culture in EoC, the generated stable epidermis presents distinct basal, spinous, granular, and cornified layers, forming a barrier function that can be detected through SDS exposure testing. We tested the irritation and penetration properties of four chemicals: isopropanol, (a liquid non-irritant), 1-bromohexane (a liquid irritant), glycerol (a semi-solid non-irritant), and cyclamen

aldehyde (a semi-solid irritant). Finally, we also tested the whitening effect of a cosmetic and demonstrated its efficacy in reducing melanin synthesis. The results indicate that the proposed organotypic physiological chip could provide an alternative for ex vivo evaluation of skin irritation or penetration, as well as for cosmetic evaluation. It is expected that EOCs will be equally important to the pharmaceutical industry, and having more human-relevant in vitro evaluation models at an early stage of drug development will improve the predictive power, thus allowing researchers to make more accurate decisions.

## Materials and methods

### *Fabrication, assembling, and operation of a microfluidic device*

The design of a microfluidic device for EoC is shown in Figure 1(a). Briefly, the microfluidic chip is comprised of four poly (methyl methacrylate) (PMMA) layers, three sealed lids, three sealing ring, three porous membranes, and twelve right angle two-way adapters. The four PMMA layers are combined into a whole with biocompatible double-side adhesive (ARcare 90445Q, Adhesives Research). Each chip contains three culture units. Every unit contains an apical inlet, an apical outlet, an apical chamber, apical microfluidic channels, a basal inlet, a basal outlet, a basal chamber and basal microfluidic channels. The apical chambers and basal chambers of the culture unit are separated by track-etched polyethylene terephthalate (PET) membranes (ipCellCulture, it4ip, Belgium) with a 1  $\mu\text{m}$  pore size and a pore density of  $2 \times 10^6$  pores per  $\text{cm}^2$ , this porous membrane supports organotypic culture while allowing efficient transport of nutrients and metabolites but prevent undesired cell migration. The apical chamber is covered by totally transparent lids, which can help observe the culture process in situ, as well as test solid or semi-solid chemicals directly or take out the organotypic tissues for further investigation. All the microfluidic channels are 0.5 mm in height and 0.5 mm in width, fabricated by computer numerically controlled (CNC) (VF-2-V, HAAS, USA) micro-milling. The chip, tubes, bottles were sterilized with ethylene oxide, then assembled in a vertical clean bench. All fluid loading and perfusion were controlled by a peristaltic pump (BT100-1L, Longer).

### *Cell culture of primary human keratinocytes and melanocytes*

Normal human keratinocytes (NHK) and normal human melanocytes (NHM) were obtained by the 0.25% w/v trypsin dermis/epidermis separation method, as our previous study,<sup>18</sup> using surgical foreskin samples from circumcised children which were kindly provided by professor Yun Zhou, Suzhou Children’s Hospital. Human juvenile

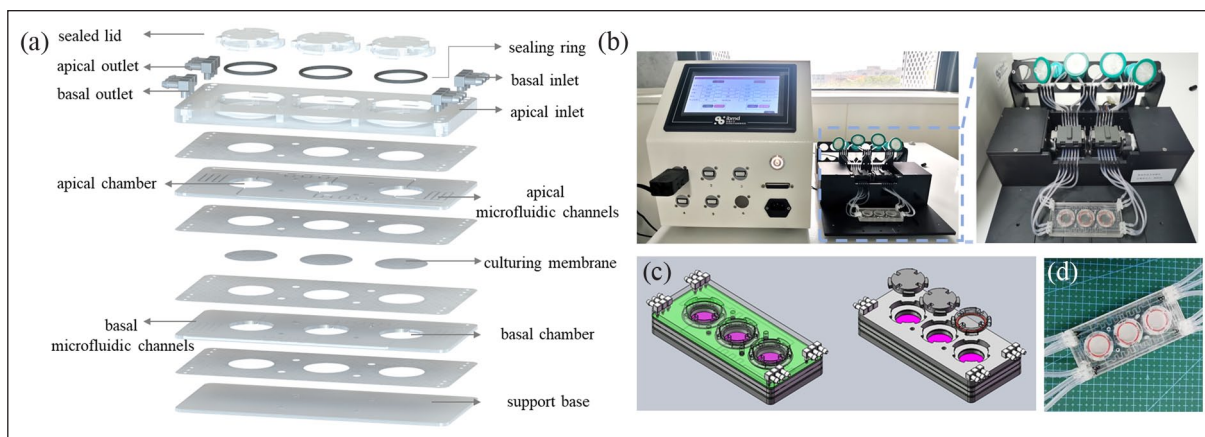


**Figure 1.** Structure of the epidermis-on-a-chip (EoC) design: (a) expanded view of the EoC, including 12 inlets, four bases, three chambers, and three sealed lids; (b) EoC dynamic culturing under the microfluidic system; (c) schematic of opening and closing the chip lids; and (d) real picture of EoC and microfluidic tubes.

prepuce after routine circumcisions from pediatric surgery was obtained in compliance with the relevant laws, and all experiments followed institutional guidelines, with informed consent and ethical approval from the Suzhou Children's Hospital. Firstly, skin samples were cut into 0.5 cm<sup>2</sup> pieces and left in 0.25% w/v trypsin overnight at 4°C. The epidermis was then excised before the papillary surface of the dermis and was gently scraped to remove basal keratinocytes and melanocytes, harvested by centrifugation (200g for 5 min). The keratinocytes in resuspension attached to culture dishes pre-coated by collagen IV and maintained in a basal serum-free medium of DMEM and F12 3: 1 supplemented with 10% v/v bovine pituitary extract, 10 ng mL<sup>-1</sup> epidermal growth factor (EGF), 0.4 μg mL<sup>-1</sup> hydrocortisone, 1.8 × 10<sup>-4</sup> M adenine, 5 μg mL<sup>-1</sup> insulin, 2 × 10<sup>-9</sup> M triiodothyronine, 5 μg mL<sup>-1</sup> transferrin and 1% v/v penicillin-streptomycin. Meanwhile, the primary cultures of melanocytes were separated by Medium 254 (Gibco, USA) supplemented with Human Melanocyte Growth Supplement (Gibco, USA).

The mixed medium of EoC with melanocytes was prepared according to the proportion of keratinocytes and melanocytes (usually 10:1<sup>19</sup>). The medium used in ALI culture is supplemented additionally with 1.2 mM calcium. Cultures were incubated at 37°C in a 5% CO<sub>2</sub> atmosphere and the culture medium were changed three times a week. Cells were passaged at 60%–80% confluence and cryopreserved in liquid nitrogen and used within six passages. All the reagents were purchased from ThermoFisher Scientific.

### Generation of EoC

First, through these three apical inlets keratinocytes suspension was added into apical chambers, approximately 6 × 10<sup>5</sup> cells per chamber, with 10% melanocytes when culture melanin model. The entire microfluidic system was

connected after the cell attachment, and the culture medium (same as in cell proliferation) was supplied to the device through a sterile syringe filter with a pore size of 0.22 μm from the medium reservoir. Then the medium flowed into the culture unit through three chambers and circularly perfused at a flow rate of 1.0 μL min<sup>-1</sup>.

After 2 days, it was transferred to ALI culture by stopping the medium perfusion of the apical chamber and pumping air at a flow rate of 1 μL min<sup>-1</sup> instead, and the perfusion medium of the bottom chamber was changed to medium containing high calcium (1.8 mM) to promote keratinocyte differentiation, stratification and cornification. After 14 days of ALI cultured, the EoC skin was used for testing or fixed.

The static skin was cultured in Transwell (Corning, USA) and fixed on the 14th day of ALI cultivation. And human skin was fixed after the epidermal layer was separated by enzymatic method.

### Treatment with test chemicals and cell viability

Four chemicals in the test were administered topically as described in OECD 439 standards,<sup>20</sup> which is an in vitro procedure that may be used for the hazard identification of irritant chemicals (substances and mixtures) in accordance with the United Nations (UN) Globally Harmonized System of Classification and Labelling (GHS) Category 2. It is based on reconstructed human epidermis (RhE), which in its overall design closely mimics the biochemical and physiological properties of the superficial layers of the human skin. In brief, EoC after 14 days full differentiation was added 10 μL of the dosing solutions, each sample was added to the chip through microfluidic tubes or top holes. The chemicals were washed off with 25 mL PBS after 15 min contact, then the chips were incubated in a humidified atmosphere at 37°C with 5% CO<sub>2</sub> and recirculated

with culture medium. 42 h after the chemical treatment, the samples were collected for analysis. Chemicals were selected based on toxicity according to the UN GHS.

Cellular viability was assessed using 3-(4,5-dimethylthiazol-2-yl)-2,5 diphenyl tetrazolium bromide (MTT, Sigma-Aldrich). Briefly, samples were washed three times in PBS, then 50  $\mu\text{L}$  MTT solution (0.5  $\text{mg mL}^{-1}$  MTT) were perfused through the apical channels and incubated for 3 h in the incubator statically. Then 1 mL iso-propanol was circularly perfused through both the apical and basal channels overnight to release the purple-colored formazan salt from living cells. Optical absorbance at 540 nm was then measured using a microplate-reader (ThermoFisher GO, USA). PBS was set as the negative control and 5% w/v SDS was set as the positive control. Cell viability ( $P_c$ ) values of the samples were calculated using the equation below:

$$P_c \% = \frac{C_d - C_c}{C_n - C_c} \times 100$$

where,  $C_d$ ,  $C_n$ , and  $C_c$  correspond to the value of the dose, negative control and positive control, respectively.

All the tests took three repetitions while in the multi-chamber chip, each group contains three repetitions. The data were used when the negative control value meets the acceptance criteria if the mean optical density (OD) value of the three replicated specimens is  $\geq 0.8$  and  $\leq 1.5$  at 570 nm using a filter band pass of maximum  $\pm 30$  nm and the positive control data meet the acceptance criteria if the mean viability is  $< 40\%$  (expressed as % of the negative control), each of the standard deviation (SD) values is considered as valid if it is  $\leq 18\%$  in the same batch. According to OECD 439,<sup>20</sup> the test substance has irritation (I) when  $P_c$  is under 50%, while it has no irritation (NI) if  $P_c$  is over 50%.

### Histological and immunofluorescence analysis

Keratinocyte cells and EoC cultured skin samples were fixed in 10% w/v neutral buffered formalin, then EoC was cut down along the edge and embedded in paraffin. EoC was sliced and deparaffinized sections of 5 microns for hematoxylin–eosin (HE) staining and immunofluorescence analysis. Caseviewer software was used to measure histological features. For immunofluorescence staining, the dewaxed and rehydrated specimens were rinsed in PBS and blocked in 0.5% v/v bovine serum albumin (BSA) containing 0.025% v/v Triton-X-100 for 1 h at room temperature (RT), then they were incubated with primary antibodies including mouse anti-keratin 10 (Abcam, USA), rabbit anti-keratin-14 (Abcam, USA), rabbit anti-loricrin (Abcam, USA), mouse anti-involucrin (Abcam, USA), rabbit anti-filaggrin (Abcam, USA), mouse anti-ZO-1 (Abcam, USA), and rabbit anti-MiTF (Abcam, USA) for 1 h. After washing

three times with PBS, the samples were incubated with secondary antibodies: goat anti-rabbit IgG conjugated to Alexa Fluor 488 (Invitrogen, USA), goat anti-mouse IgG conjugated to Alexa Fluor 546 (Invitrogen, USA), and donkey anti-mouse IgG conjugated to Alexa Fluor 488 (Invitrogen, USA) for 1 h at RT. Slides were incubated with 4',6-diamidino-2-phenylindole (DAPI) (ThermoFisher Scientific, USA) and examined using a fluorescent inverted microscope (IX-83, Olympus, Japan), fluorescence images were analyzed using ImageJ software.

### Live/Dead assay

The Live/Dead assay kit (Invitrogen, USA) was used for live/dead staining on the day 7. After 15 min of incubation with the staining solution (Calcein AM/ iodide: DMEM / 10% v/v FBS=1:1), the samples were washed for three times in PBS and viewed on an inverted fluorescence microscope (IX-83, Olympus, Japan) at an excitation and emission wavelength of 488 nm and 515 nm for green (live) while 570 and 602 nm for red (dead).

### Paracellular permeation

To examine the permeability, the samples were perfused with a 607 Da Cascade Blue solution (50  $\mu\text{M}$ ) and 70 kDa Texas Red solution (10  $\mu\text{M}$ ) and detected at 4 h. Briefly, each sample was prefilled with 50  $\mu\text{L}$  PBS in the bottom chamber of the chip or culture dish. A 50  $\mu\text{L}$  permeating solution was then added to the top of the samples and incubated at 37°C.

At the detection point, 50  $\mu\text{L}$  of the solution from the bottom of the insert was moved into a 96-well plate. Then, the quantities of collected dextran were measured using a microplate reader (ThermoFisher Scientific GO, USA) at an excitation and emission wavelength of 355 and 460 nm for Cascade Blue while 544 and 590 nm for Texas Red. A permeating standard curve was plotted at fluorescence concentrations of 0.001, 0.005, 0.01, 0.05, and 0.1  $\text{mg mL}^{-1}$ .

Finally, the percentage of the dextran permeability ( $P_{app}$ ) values of the samples were calculated using the equation below:

$$P_{app} = \frac{J}{A \times \Delta C}$$

$J$  is the molecular flux,  $A$  is the total area of diffusion, and  $\Delta C$  is the average gradient, respectively.

### Transdermal permeation

All the samples were tested by liquid Chromatograph Mass Spectrometer (LC-MS) method, using an Agilent 1100 series HPLC with Eclipse Plus C18, 2.1  $\times$  150 mm,

3.5  $\mu\text{m}$  column. And the MS used Thermo TSQ Quantum Ultra (ESI ion source), the ion spray voltage was 3000 KV. Three EoC samples, and three it4ip membranes were fixed in a vertical diffusion, and the cuticle is the medicated surface. The pool shall be in close contact with the receiving fluid (no bubbles). The receiving pool was added with drained bubble receiving solution (sterile normal saline). 10 mg of standard prednisone acetate was added into a 100 mL volumetric flask, and the volume was fixed with methanol to prepare 100  $\mu\text{g}/\text{mL}$  prednisone acetate methanol solution, and 20 mL prednisone acetate methanol solution was diluted twice with the same volume of normal saline. Then 2 mL of 50  $\mu\text{g}/\text{mL}$  prednisone acetate solution was added into the drug delivery pool, and we sealed the drug delivery pool with a sealing film. The diffusion instrument has a constant temperature ( $37.0 \pm 0.5^\circ\text{C}$ ), a magneton rotation speed of 100 R/min, and an effective diffusion area of 2.2  $\text{cm}^2$ . 0.5 mL of the samples were collected at 2, 6, and 24 h during the test, and the same volume of receiving solution was supplemented after the collection. A permeating standard curve was plotted at fluorescence concentrations of 5000, 1000, 500, 100, 50, 10, and 2 ng/mL.

Finally, the accumulative permeated amount was calculated using the equation below:

$$Q_n = C_n \times V_r + \sum_{i=1}^{n-1} C_i \times V_i$$

In the formula,  $Q$  is the accumulative permeated amount per unit area,  $V_r$  is receiving liquid volume,  $V_i$  is taking liquid volume,  $C_n$  is concentration of the sampling.

### Measurement of cosmetic whitening effects

Preparing four groups of EoC as negative control (NC), positive control (PC), test group (TG), and blank control separately (BC). The NC, PC, TG groups contained 10% melanocytes, and starting UVB irradiation from the third day, 50  $\text{mJ}/\text{cm}^2$  dose of UVB irradiation was given daily for 7 days. While, the blank control had neither melanocytes nor irradiation. On the sixth- and eighth-days, opening top lids and applying 10  $\mu\text{L}$  cosmetics (its effective ingredients including scutellaria baicalensis root extract, morus alba root extract, hydrolyzed opuntia ficus-indica flower extract) to the TG EoC, and added 10  $\mu\text{L}$  0.05% w/v kojic acid (Sigma-Aldrich) to the PC. EoC was photographed on day 14.  $\Delta\text{L}^*$  value was measured using Chroma Meter NR60CP (3nh, China). Melanin content was measured on days 14 by Solvable Melanin assay.<sup>21</sup> Fontana–Masson silver staining (Abcam) was used for melanin staining in paraffin-embedded tissues.

### Statistical analysis

Statistical analysis was performed using one-way ANOVA or Student's  $t$ -test with 95% confidence interval using the

software GraphPad Prism. For testing the barrier function, three skin constructs per condition were used.  $p < 0.05$  was considered significantly different. Data were shown as means  $\pm$  SEM.

## Results and discussion

### Construction of epidermis in EoC

We reconstructed skin on a tissue chip, and we named it Epidermis-on-a-chip.<sup>22</sup> The design of the microfluidic device for the EoC is shown in Figure 1(a). Briefly, the microfluidic chip is comprised of four poly (methyl methacrylate) (PMMA) layers, three sealed lids, three sealing rings, three porous membranes, and twelve right-angle two-way adapters. The four PMMA layers are combined into the chip body (see Materials and Methods). Each chip contains three culture units, where each unit contains an apical inlet, an apical outlet, an apical chamber, apical microfluidic channels, a basal inlet, a basal outlet, a basal chamber, and basal microfluidic channels. The apical chambers and basal chambers of the culture unit are separated by track-etched polyethylene terephthalate (PET) membranes, allowing for efficient transport of nutrients and metabolites while preventing undesired cell migration. The apical chamber is covered by totally transparent lids, which can help to observe the culture process in situ, as well as to test solid or semi-solid chemicals directly or remove the organotypic tissues for further investigation. Then, the EoC was linked, as shown in Figure 1(b) and (d), into a system including a microfluidic culture system and dosing windows (Figure 1(c)), which can provide a liquid or air–liquid culture environment for normal human keratinocytes (NHKs). As shown in Figure 2(a), we seeded the NHKs onto the porous membrane of the chip. After 2 days of proliferation, we provided an air–liquid atmosphere above the keratinocytes. Culturing at the air–liquid interphase resulted in a proliferating stratum basal differentiating into spinous layer and granular layer. Finally, a cornified layer was formed as the keratinocytes migrated upward (Figure 2(b) and (c)). Figure 2(d) shows that CK14 was expressed robustly, and the cells presented good morphology in Bright-field and DAPI staining images, indicating high viability. After 14 days of cell differentiation, the Live/Dead staining images (Figure 2(e)) indicated that the cells maintained relatively high viability, as few dead cells were observed in the scope.

### Differentiation of epidermis

To analyze the morphology and characterization of the EoC, we evaluated cryo-sections of EoC samples and human native skin through HE staining and immunostaining. As shown in Figure 3(a), compared with static skin, the EoC skin differentiation was more pronounced. In particular, the cells of the basal layer were arranged more tightly, and the thickness was approximately over 50  $\mu\text{m}$ ,

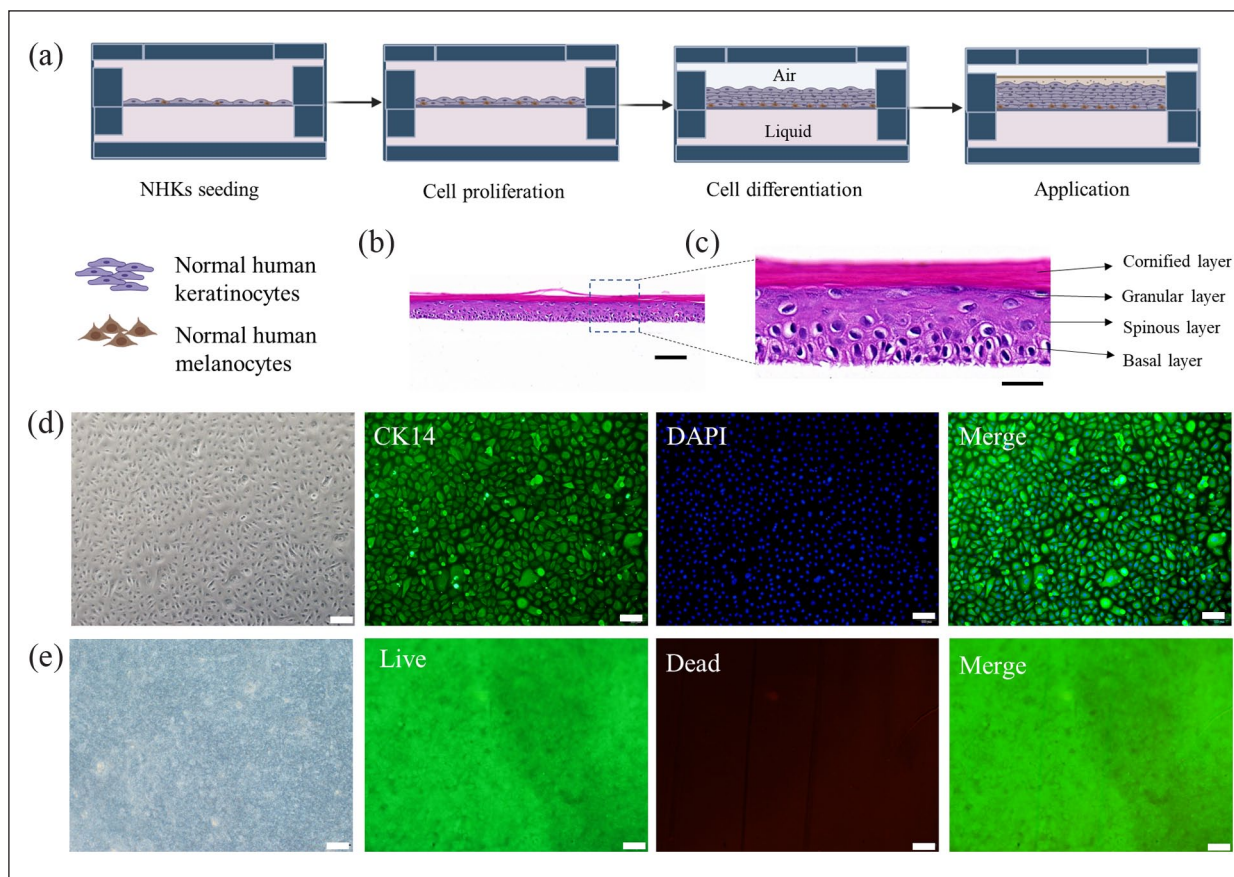


**Figure 2.** Cell isolation and skin cell growth: (a) schematic of normal human keratinocytes and melanocytes culture on the chip and cell differentiation in the air (blue) and liquid (pink) environments; (b) HE staining picture of EoC cultured for 14 days; (c) partially enlarged detail of (b and d) representative images of immunofluorescence staining of primary human keratinocytes. Images of keratinocytes show positive expression of cytokeratin 14 (green). Cell nuclei were stained with DAPI (blue); and (e) Live/Dead staining fluorescence images after 14 days of cell differentiation. Scale bar: (b) 100  $\mu\text{m}$ ; (c) 25  $\mu\text{m}$ ; (d and e) 100  $\mu\text{m}$ .

structurally similar to the human native skin sample. For comparison, a commercial skin equivalent (EpiDerm™, MatTek Corp., Ashland, MA, USA) presented a thickness of 28–43  $\mu\text{m}$ .<sup>23</sup> This indicates that the reconstructed skin in the microfluidic system underwent an enhanced differentiation process. Additionally, the resulting epithelium had well-organized basal cells adhering to the PET base membrane, indicating the development of mature skin. Besides providing a continuous supply of nutrients and removal of metabolic wastes, microfluidic perfusion likely increased the shear stress, which can drive epidermal maturation<sup>24</sup> and modulate its biological barrier function.<sup>25</sup>

As shown in Figure 3(b), CK14 and CK10 were localized to the basal layer and the cornified layer, respectively, indicating that differentiation had been induced in the epidermal layers on the EoC.<sup>15</sup> The presence of an orthokeratinized cornified layer and the expression of cornified envelope proteins is one of the hallmarks of epidermal differentiation.<sup>25</sup> Similar to human native skin, the EoC sample demonstrated positive expression of loricrin, filaggrin, and involucrin, as shown in Figure 3(b). The late

differentiation marker loricrin was continuously and intensely distributed in the granular layer, suggesting advanced cell differentiation in the EoC. The similar expression levels of filaggrin and involucrin, when compared to native skin, also indicated epidermal homeostasis. Taken together, these features demonstrated successful reconstruction of a morphologically superior model under microfluidic culture conditions. We believe that the advanced differentiation and strong expression of key hallmark proteins are related to enhanced barrier functions.<sup>26</sup>

### Barrier function of the EoC

The skin's most important function is to form an effective barrier between the organism and the environment, preventing invasion by pathogens and fending off chemical and physical assaults.<sup>27</sup> The stratum corneum serves as the principal barrier against the percutaneous penetration of chemicals and microbes<sup>27,28</sup> and consists of protein-enriched cells (i.e. corneocytes embedded in a lipid matrix). It is located at the end of the keratinocyte

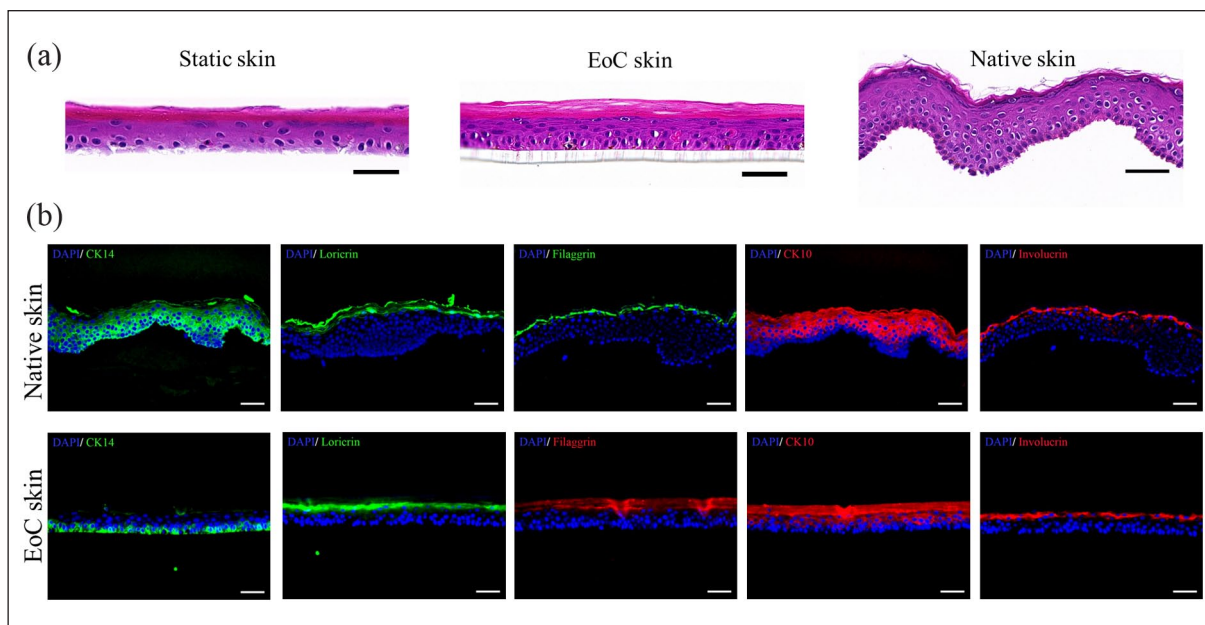


**Figure 3.** Skin HE staining and immune staining: (a) Representative images of HE staining of static skin, EoC skin, and human skin after 14 days of in vitro maturation. The static skin was cultured in Transwell plates and incubated in a static environment, EoC skin was dynamically cultured in microfluid environment. Both were air–liquid interface (ALI) cultured for 14 days. The native skin was derived from child foreskin tissue; and (b) representative images of immunofluorescence staining of human native skin and EoC after 14 days of in vitro maturation. Images of EoC show positive expression of cytokeratin 14 (green), loricrin (green), filaggrin (green for native skin and red for EoC), cytokeratin 10 (red), and involucrin (red), similar to native skin. Cell nuclei were stained with DAPI (blue). Scale bar: (a and b) 50  $\mu$ m.

differentiation and is well-known to contribute to the skin barrier function.<sup>8</sup> We assessed the permeability of different fluorescent molecule solutions to evaluate the resistance to external substances. These experiments were conducted in situ. The original fluorescent solution was added to the upper chamber from the corresponding flow channel, and the fluorochrome flux through the skin equivalents were measured by collecting the supernatant from the basal chamber (or insert reservoir) and reading the fluorescence signals (which is correlated to the fluorochrome concentration). The results demonstrated that the EoC could prevent the permeation of both cascade blue (607Da) and Texas red (70 kDa) significantly (Figure 4(a)); in particular, it blocked 99.83% of the small-molecule fluorochrome.

Tight junctions (TJs) are another barrier structure of the skin, which reside immediately below the stratum corneum and regulate the selective permeability of the paracellular pathway.<sup>29</sup> TJs are composed of three structural transmembrane components: the IgG-like family of junctional adhesion molecules (JAMs), the claudin family molecules, and the occludin family molecule (the latter two comprising four transmembrane-spanning molecules).<sup>30</sup> In addition, several scaffolding proteins, such as zonula occludens (ZO)-1, ZO-2, ZO-3, multi-PDZ domain protein 1, membrane-associated guanylate kinase, and cingulin, have been identified in the TJ cytosolic plaque,<sup>29</sup> and either ZO-1 or ZO-2 (but not ZO-3) is crucial

for clustering of claudins, strand formation, and barrier function, and have been widely used for epithelial<sup>31</sup> or endothelial<sup>32</sup> TJ evaluation. ZO-1 was distinctly expressed in the constructed epidermis under the stratum corneum (Figure 4(b)), which was constant with respect to the fluorescent penetration detection.

Additionally, we characterized the skin barrier function after SDS exposure, according to a static in vitro skin model test.<sup>20</sup> As described in OECD439, the stratum corneum and its lipid composition should be sufficient to resist the rapid penetration of cytotoxic benchmark chemicals, such as SDS or Triton X-100, as estimated by the  $IC_{50}$  or  $ET_{50}$ . High concentration SDS is typically used as a negative control, where a low concentration but long-time exposure could indicate external substance prevention. As shown in Figure 4(c), more than half of the tissue cells remained alive after an 18 h exposure to 2 mg/mL SDS (0.2% m/v), which satisfied the recommendation of OECD439; namely, the lower acceptance limit is 1.0 mg/mL and the upper acceptance limit is 4.0 mg/mL.<sup>20</sup> Further cell viability detection by MTT (Figure 4(d)) supported this conclusion, where the  $IC_{50}$  could be estimated by determination of the concentration at which a benchmark chemical reduced the viability of the tissues by 50% after a fixed exposure time. For a static in vitro skin model, only the batch satisfying the release criteria can be used for further application (e.g. irritation or photo-toxicity assessment).

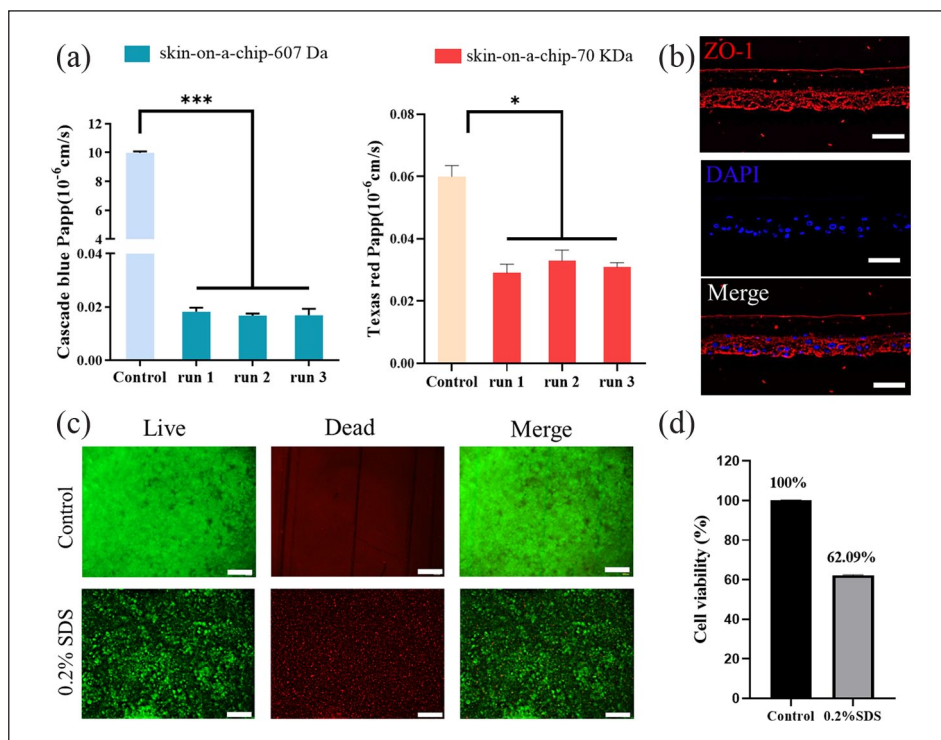


**Figure 4.** Skin permeability of fluorescence dyes and barrier function: (a) Two fluorescence dyes—Cascade Blue (607 Da) and Texas Red (70 KDa)—were compared between EoC and control (it4ip porous membrane) after 4 h of cumulative permeability, repeated three times. Statistical analysis was performed using one-way ANOVA analyses: \* $p < 0.05$ ; \*\* $p < 0.01$ ; \*\*\* $p < 0.001$ ; (b) skin slices were stained with ZO-1 (red) and DAPI (blue); (c) Live/Dead staining fluorescence images before and after 0.2% w/v SDS treatment; and (d) cell viability bar chart of before and after 0.2% w/v SDS treatment. Scale bar: (b) 50  $\mu\text{m}$ ; (c) 100  $\mu\text{m}$ .

Epidermal barrier function and the related field of percutaneous absorption have been actively investigated in the pharmaceutical and cosmetics fields, as the skin acts as the body's first line of defense against infection, temperature change, and other challenges to homeostasis.<sup>33</sup> From the recognition that the stratum corneum is the principal barrier according to recent research on TJs, the barrier function of the skin is a key line of investigation in both academia and industry, indicating the importance of percutaneous penetration testing. Trans-epithelial electrical resistance (TEER) has been broadly used for barrier function evaluation, being a quick, conventional, and non-invasive assay to evaluate the integrity and differentiation of in vitro epithelial monolayers and tissues, for which the integration of sensors (e.g. varied electrodes) is a key advantage of organ-on-a-chip technologies.<sup>5,34</sup> Ultimately, a more sophisticated understanding of the epidermal barrier function may lead to more biomimetic in vitro skin models and more rational methods for the application of such models.

#### Para-cellular permeation of prednisone acetate

Glucocorticoids are steroid hormones which are excreted from the adreno-cortex in accordance with the circadian

rhythm. They are not only important in regulating the biosynthesis and metabolism of sugar, fat, and protein, but also in protecting against stress, shock, inflammation, and so on.<sup>35</sup> Due to their powerful anti-inflammatory and immunosuppressive properties, glucocorticoids have become commonly used drugs in the treatment of autoimmune and acute and chronic inflammatory diseases. PA is an important glucocorticoid drug,<sup>36,37</sup> which can be taken orally, applied to the skin, injected locally, or dropped into the conjunctival sac. In this work, we tested the effects of PA on the skin using a permeation treatment.

As shown in Figure 5(a), PA solution (50  $\mu\text{g}/\text{mL}$ ) was applied to control and EoC skin for 24 h, and the permeation concentrations of PA in the receive pool for control and EoC groups increased linearly with different slopes over time. The control group presented the highest accumulative permeated amount (APM), about  $0.508 \pm 0.014 \mu\text{g}/\text{cm}^2$  at 24 h, and the concentration was 1136.11 ng/mL (the peak area is shown in Figure 5(bii)), with 7.43% accumulative permeated rate. Meanwhile, the accumulative permeated rate of the EoC group was about 0.36% less than that of the control, and the APM was  $0.133 \pm 0.015 \mu\text{g}/\text{cm}^2$  at 24 h (the peak area is shown in Figure 5(bi)).

In brief, the in vitro skin samples cultured by EoC presented effective barrier function, thus providing a potential

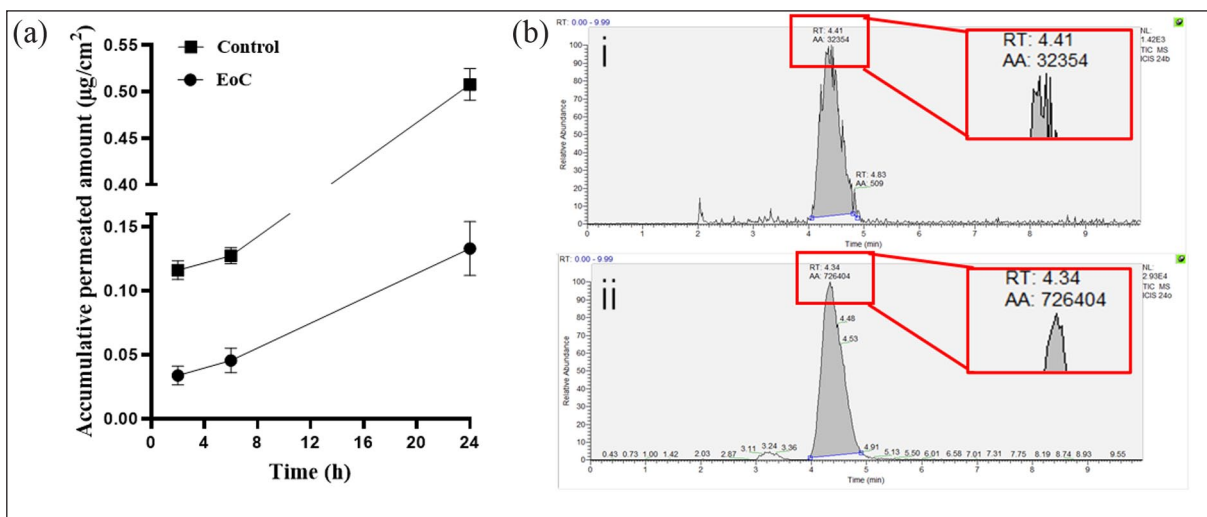


**Figure 5.** EoC Tests with Transdermal Diffusion System and Materials Detected by LC-MS: (a) three EoC samples and three it4ip porous membranes (control) were fixed for vertical diffusion, and the cuticle was the medicated surface. The prednisone acetate (PA) accumulative permeated amount was tested at 2, 6, and 24 h for LC-MS detection; (b) MS pictures of (i) EoC and (ii) control (it4ip porous membranes) at 24 h. NL, normalized level; RT, retention time; AA, automatic integration area.

model for percutaneous improvement of drugs such as PA with limited skin penetration ability, making them unsuitable for transdermal drug delivery. Although the transdermal delivery of drugs is an appealing method, not all glucocorticoid drugs are appropriate for the transdermal dosage route, due to the inherent constraint of transdermal drug absorption, as regulated by the stratum corneum (outermost layer of the skin).<sup>38</sup> Therefore, improving the permeability of drugs is a valuable research direction; for example, a previous study has indicated that mixing a drug into a gel could provide a potential drug delivery method.<sup>39,40</sup>

### Evaluation of skin irritation

Due to legal and ethical demands, the construction and application of *in vitro* engineered skin models has gained attention over the past four decades. Since the 1980s, various reconstructed epidermis models have been developed and used for skin irritation testing. For the detection and quantification of irritants and non-irritants, EpiSkin™ and EpiDerm™ have passed through the whole validation process.<sup>41</sup> Different from these static skin models, skin-on-a-chip systems can achieve dynamic culture, but still require manual operation for drug screening or cosmetics detection, especially when considering pumpless skin-on-a-chip.<sup>11,12</sup> Meanwhile, pump-driven EoC technology is convenient for automatic detection in this context; however, most such chips utilize culture chambers enveloped by the chip substrate, making them unsuitable for pasty or semi-solid sample loading, which are common in cosmetics. In general, the pasty or semi-solid samples will block the microfluidic pipeline, making it difficult to precisely

control the sample loading amount. At the same time, a large amount of liquid and time are required for cleaning after sample addition, affecting the detection efficiency of the chip. The chip designed in this work includes detachable lids, which can be sealed during culture and removed when loading samples (Figure 1(c)). Before loading, the lids are taken down with a purpose-built tool, following which liquid or solid reagents can be added using through pipettor or pipette. Finally, the lids are recovered to the chambers after sample exposure.

We detected four chemicals, as illustrated in Figure 6(b) and (c): two non-irritant chemicals, isopropanol (liquid) and glycerol (viscid) and two irritant chemicals, 1-bromohexane (liquid) and cyclamen aldehyde (viscid). Glycerol and cyclamen aldehyde are pasty and, so, a large amount of buffer solution is typically required to wash them after exposure in traditional OOC models; however, with the proposed EoC, we could wash them away with the help of peristaltic pumps. According to OECD439, the test chemical was identified as requiring classification and labeling; according to UN GHS (Category 2 or Category 1), a chemical is an irritant if the mean percent tissue viability is less than or equal ( $\leq$ ) to 50%, and it may be considered as a non-irritant to skin when the tissue viability is above the defined threshold level. To guarantee the validity of the detection, a negative control and positive control were concurrently used in each run. PBS and 5% w/v SDS were chosen in this work, and it was found that the barrier function and tissue sensitivity of the EoC were within the defined acceptance range (Figure 6(a)). As a result, the detection test accurately predicted irritants and non-irritants. Generally, a sensitivity of 80%, specificity of 70%, and accuracy of 75% could be considered as indicating an adequate skin model

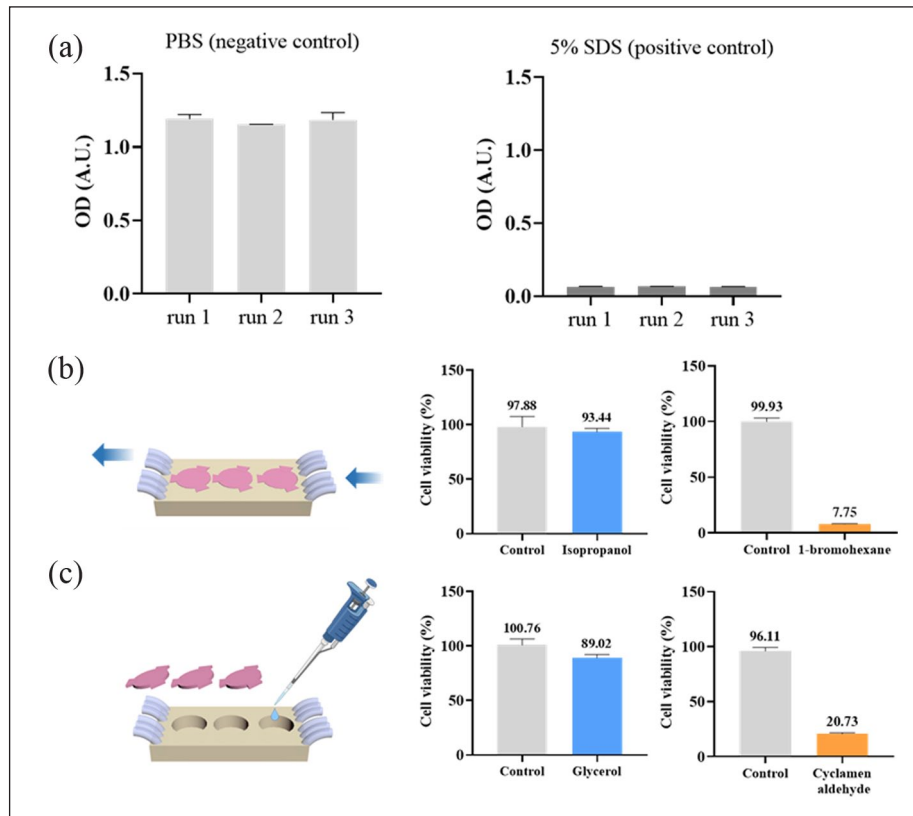


**Figure 6.** Skin with four different chemical interferences: (a) the absorbance of negative (PBS) and positive (5% w/v SDS) controls, repeated three times; (b) through the microfluidic tubes, isopropanol and 1-bromo-hexane were loading into the chip, maintained about 15 min, then washed with PBS. Bar charts show the cell viability results for the experimental and control groups; (c) the lids were removed to add the semi-solid samples—glycerol and cyclamen aldehyde—to the surface of the EOC. After stimulation had ended, the EOC surface was cleaned, the lids were tightened, and culturing was continued. Bar charts show the cell viability results for the experimental and control groups.

for irritation testing (e.g. Episkin™, which has been used for detection of more than 20 chemicals in three laboratories, achieved a sensitivity of 90%, specificity of 90%, and accuracy of 85%<sup>41</sup>). We still need to conduct more tests with various chemicals, as well as in different labs, in order to validate the results provided in this study.

Besides sample loading, the detachable lid design could be changed into Franz diffusion cell like lids, used in static percutaneous penetration testing. Previous research has even shown that the use of a physiological platform could decrease the effect of unstirred water layers, which can occur in static Franz cells.<sup>42</sup> Additionally, we could achieve high-throughput detection by repeated use of the triple-unit, as well as obtaining either series-wound or shunt-wound chips through use of a flow-in pipe option.

### Whitening effect of cosmetics

The skin is an important organ that protects the human body from ultraviolet radiation (UVR). Over-expression of melanin may lead to certain skin diseases, such as melasma,<sup>43</sup> while declining pigmentation has become a research hot spot in the field of medicine.<sup>44</sup> Meanwhile,

whitening cosmetics have become more and more attractive to the public, due to beauty and health concerns. Therefore, we applying 10  $\mu$ L cosmetics (a developing cosmetic ingredient from a Chinese company), and set kojic acid as the positive control, in order to demonstrate that the EoC has potential for real market application in the future.

As Figure 7(a) shows, the normal human melanocytes (NHM) produced significant melanin and expressed melanocyte-specific proteins, such as Mitf.<sup>45</sup> After 14 days of ALI culture with the EoC, Figure 7(b) demonstrates that the EoC skin was obviously differentiated and expressed melanin particles. Subsequently, after treatment with the cosmetic, the apparent chroma (Figure 7(c)) of TG was more visibly shallowed than NC, and similar to that of PC. Compared with BC, there is no doubt that NC presented obvious melanism. The L\* value (Figure 7(d)) and melanin content (Figure 7(g)) indicated that TG presented a significant difference from NC, and the standard deviation of 3 TG samples was less than 3%, demonstrating that the test has good repeatability. Then, to detect visible melanin in tissues on day 14, Fontana–Masson staining (Figure 7(e)) was applied. The results indicated that the melanin content and distribution were visibly decreased in the PC,

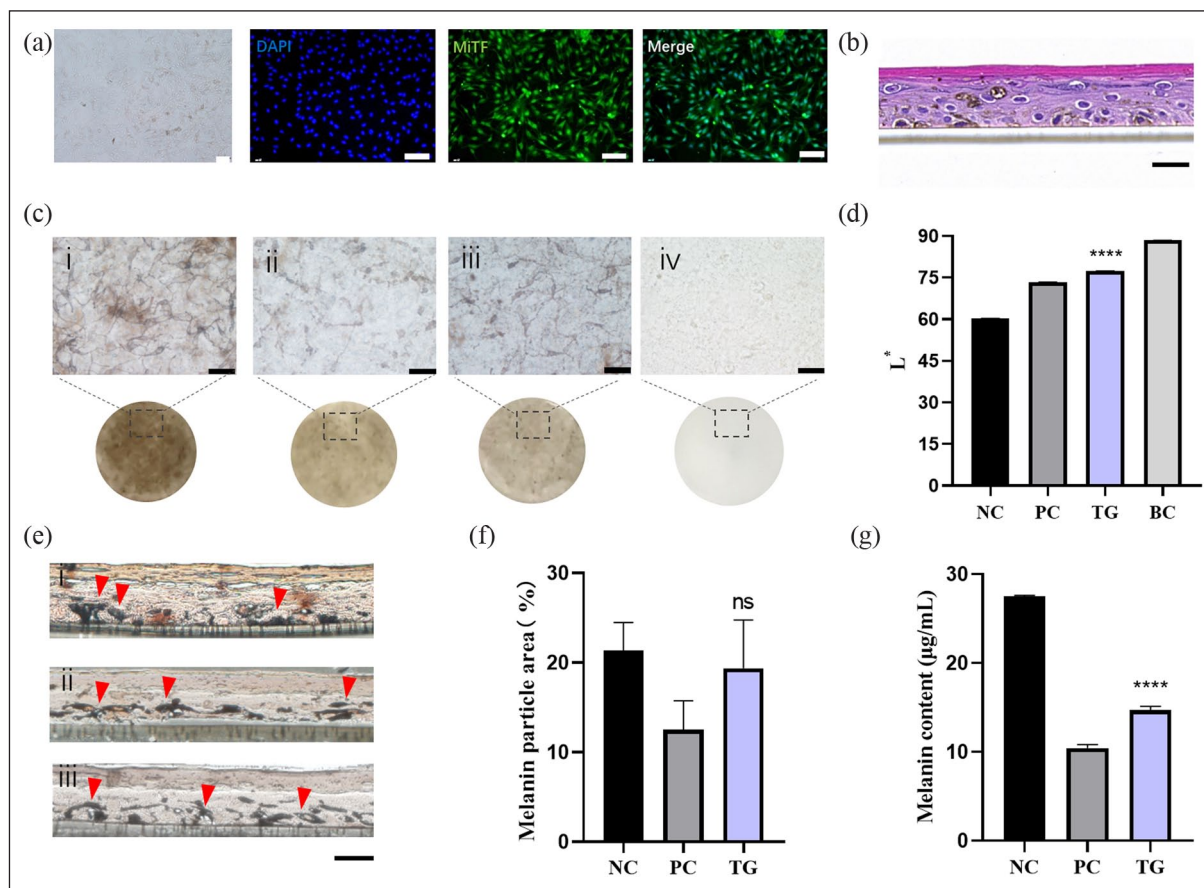


**Figure 7.** Cosmetics whitening test on EoC: (a) Optical and cell nucleus (blue) and MITF (green) immunofluorescence images of normal human melanocytes; (b) HE staining image of EoC including melanocytes after 14 days of ALI culture; (c) optical images of EoC after 14 days of ALI culture and cosmetics treatment: (i) negative control (NC), (ii) positive control (PC), (iii) test group (TG), and (iv) blank control separately (BC); (d) bar chart of L\* statistics; (e) Masson–Fontana staining of EoC paraffin section: (i) NC, (ii) PC, (iii) TG; (f) statistical bar chart of melanin particle area for the three groups; and (g) melanin content bar chart for the three groups. Scale bar: (a) 100 µm; (b and c) 50 µm; (e) 50 µm. All tests were repeated three times. The NC group and the TG were analyzed using one-way ANOVA test: \* $p < 0.05$ ; \*\* $p < 0.01$ ; \*\*\* $p < 0.001$ ; \*\*\*\* $p < 0.0001$ .

compared with NC, after treatment with kojic acid, whereas the melanin particle area of TG presented an insignificant decrease, compared with NC, of about 19.39% (Figure 7(f)). These results indicate that the whitening mechanisms of the tested cosmetic are complicated,<sup>46,47</sup> likely contributing to the inhibition of melanin expression and transport, as well as preventing pigmentation. Similar mechanisms have been inferred in previous cosmetics ingredient studies; for example, some natural ingredients, such as  $\alpha$ -arbutin<sup>48</sup> and resveratrol<sup>49</sup> have been shown to decrease TYR activity to reduce melanin production, while Argan Press Cake (APC)<sup>50</sup> and nicotina-mide<sup>51</sup> inhibited melanin transport.

## Conclusion

We designed a simple, functional, and repeatable EoC, whose usable tissue is a cornified epidermis. The reconstructed skin of the EoC features complete differentiation, as verified by the expression levels of signature

proteins. The favorable barrier function of the chip was demonstrated to be suitable for application in irritation evaluation and preliminary permeation detection; in particular, the detachable lid facilitates the loading of solid or semi-solid samples. Meanwhile, the proposed EoC can also be considered a reasonable choice for evaluating the effectiveness of cosmetics, in terms of aspects such as corrosiveness, phototoxicity, and whitening. Furthermore, the EoC skin, as a simulated skin model, could be popularized for application in the cosmetics and pharmaceutical industries, in order to better evaluate products. Meanwhile, the EoC, as a culture unit, could be easily expanded into a multi-unit chip, due to the use of a pump-based physiological system, thus providing a potential strategy to achieve high-throughput testing, which is urgently needed for the effective measurement of skin irritation, penetration, or other skin evaluation indices, which may efficiently improve the development of the pharmaceutical and cosmetic industries.

## Declaration of Conflicting Interests

The author(s) declared no potential conflicts of interest with respect to the research, authorship, and/or publication of this article.

## Funding

The author(s) disclosed receipt of the following financial support for the research, authorship, and/or publication of this article: This work was supported by the National Key R&D Program of China (Grant No. 2017YFA0700500), the Natural Science Foundation of Jiangsu Province (Grant No. BK20190192), the Experiment Project of China Manned Space Program (Grant No. HYZHXM01019), the Fundamental Research Funds for the Central Universities from Southeast University (Grant No. 3207032201A3), and the People's Livelihood Science and Technology Project of Suzhou (Grant No. SS202013).

## ORCID iD

Zaozao Chen  <https://orcid.org/0000-0001-8922-370X>

## References

1. Yu F, Selva Kumar ND, Choudhury D, et al. Microfluidic platforms for modeling biological barriers in the circulatory system. *Drug Discov Today* 2018; 23: 815–829.
2. Moniz T, Costa Lima SA and Reis S. Human skin models: from healthy to disease-mimetic systems; characteristics and applications. *Br J Pharmacol* 2020; 177: 4314–4329.
3. Van Gele M, Geusens B, Brochez L, et al. Three-dimensional skin models as tools for transdermal drug delivery: challenges and limitations. *Expert Opin Drug Deliv* 2011; 8: 705–720.
4. van den Broek LJ, Bergers LIJC, Reijnders CMA, et al. Progress and future perspectives in skin-on-chip development with emphasis on the use of different cell types and technical challenges. *Stem Cell Rev Rep* 2017; 13: 418–429.
5. Zhang Q, Sito L, Mao M, et al. Current advances in skin-on-a-chip models for drug testing. *Microphysiol Syst* 2018; 2: 4.
6. Pires de Mello CP, Carmona-Moran C, McAleer CW, et al. Microphysiological heart-liver body-on-a-chip system with a skin mimic for evaluating topical drug delivery. *Lab Chip* 2020; 20: 749–759.
7. Lee JH and Kim HW. Emerging properties of hydrogels in tissue engineering. *J Tissue Eng* 2018; 9: 2041731418768285.
8. Mathes SH, Ruffner H and Graf-Hausner U. The use of skin models in drug development. *Adv Drug Deliv Rev* 2014; 69–70: 81–102.
9. Huh D, Hamilton GA and Ingber DE. From 3D cell culture to organs-on-chips. *Trends Cell Biol* 2011; 21: 745–754.
10. Blumenrath SH, Lee BY, Low L, et al. Tackling rare diseases: clinical trials on chips. *Exp Biol Med* 2020; 245: 1155–1162.
11. Jusoh N, Ko J and Jeon NL. Microfluidics-based skin irritation test using in vitro 3D angiogenesis platform. *APL Bioeng* 2019; 3: 036101.
12. Kim K, Jeon HM, Choi KC, et al. Testing the effectiveness of Curcuma longa leaf extract on a skin equivalent using a pumpless skin-on-a-chip model. *Int J Mol Sci* 2020; 21: 3898.
13. Jeon HM, Kim K, Choi KC, et al. Side-effect test of sorafenib using 3-D skin equivalent based on microfluidic skin-on-a-chip. *J Ind Eng Chem* 2020; 82: 71–80.
14. Schimek K, Markhoff A, Sonntag F, et al. Integrating skin and vasculature in a multi-organ-chip platform. *BMC Proc* 2015; 9: 9.
15. Mori N, Morimoto Y and Takeuchi S. Skin integrated with perfusable vascular channels on a chip. *Biomaterials* 2017; 116: 48–56.
16. Ramadan Q and Gijs MA. In vitro micro-physiological models for translational immunology. *Lab Chip* 2015; 15: 614–636.
17. Maschmeyer I, Lorenz AK, Schimek K, et al. A four-organ-chip for interconnected long-term co-culture of human intestine, liver, skin and kidney equivalents. *Lab Chip* 2015; 15: 2688–2699.
18. Zhang J, Chen Z, Zhang Y, et al. Construction of a high fidelity epidermis-on-a-chip for scalable in vitro irritation evaluation. *Lab Chip* 2021; 21: 3804–3818.
19. Cichorek M, Wachulska M, Stasiewicz A, et al. Skin melanocytes: biology and development. *Postepy Dermatol Alergol* 2013; 30: 30–41.
20. OECD. *Test No. 439: In vitro skin irritation: Reconstructed human epidermis test method*. OECD, 2019.
21. Bessou-Touya S, Pain C, Taïeb A, et al. Chimeric human epidermal reconstructs to study the role of melanocytes and keratinocytes in pigmentation and photoprotection. *J Invest Dermatol* 1998; 111: 1103–1108.
22. Kazem S, Linszen EC and Gibbs S. Skin metabolism phase I and phase II enzymes in native and reconstructed human skin: a short review. *Drug Discov Today* 2019; 24: 1899–1910.
23. Curren R.d MG, Gibson DP and Aardema MJ. Development of a novel micronucleus assay in the human 3-D skin model, EpiDerm™. In: Presented at the 44th Annual Meeting of the Society of Toxicology, New Orleans, LA, 6–10 March 2005.
24. O'Neill AT, Monteiro-Riviere NA and Walker GM. Characterization of microfluidic human epidermal keratinocyte culture. *Cytotechnology* 2008; 56: 197–207.
25. Sriram G, Alberti M, Dancik Y, et al. Full-thickness human skin-on-chip with enhanced epidermal morphogenesis and barrier function. *Mater Today* 2018; 21: 326–340.
26. Strüver K, Friess W and Hedtrich S. Development of a perfusion platform for dynamic cultivation of in vitro skin models. *Skin Pharmacol Physiol* 2017; 30: 180–189.
27. Proksch E, Brandner JM and Jensen JM. The skin: an indispensable barrier. *Exp Dermatol* 2008; 17: 1063–1072.
28. Madison KC. Barrier function of the skin: “la raison d'être” of the epidermis. *J Invest Dermatol* 2003; 121: 231–241.
29. De Benedetto A, Rafaels NM, McGirt LY, et al. Tight junction defects in patients with atopic dermatitis. *J Allergy Clin Immunol* 2011; 127: e771773–77786.e1.
30. Niessen CM. Tight junctions/adherens junctions: basic structure and function. *J Invest Dermatol* 2007; 127: 2525–2532.
31. Leibrock L, Wagener S, Singh AV, et al. Nanoparticle induced barrier function assessment at liquid–liquid and air–liquid interface in novel human lung epithelia cell lines. *Toxicol Res* 2019; 8: 1016–1027.

32. Abdala-Valencia H, Kountz TS, Marchese ME, et al. VCAM-1 induces signals that stimulate ZO-1 serine phosphorylation and reduces ZO-1 localization at lung endothelial cell junctions. *J Leukoc Biol* 2018; 104: 215–228.
33. Blickenstaff NR, Coman G, Blattner CM, et al. Biology of percutaneous penetration. *Rev Environ Health* 2014; 29: 145–155.
34. Guo Z, Higgins CA, Gillette BM, et al. Building a micro-physiological skin model from induced pluripotent stem cells. *Stem Cell Res Ther* 2013; 4(Suppl 1): S2.
35. Alépée N, Tornier C, Robert C, et al. A catch-up validation study on reconstructed human epidermis (SkinEthic RHE) for full replacement of the draize skin irritation test. *Toxicol In Vitro* 2010; 24: 257–266.
36. Alberti M, Dancik Y, Sriram G, et al. Multi-chamber microfluidic platform for high-precision skin permeation testing. *Lab Chip* 2017; 17: 1625–1634.
37. Nozaki O. Steroid analysis for medical diagnosis. *J Chromatogr A* 2001; 935: 267–278.
38. Frerichs VA and Tornatore KM. Determination of the glucocorticoids prednisone, prednisolone, dexamethasone, and cortisol in human serum using liquid chromatography coupled to tandem mass spectrometry. *J Chromatogr B Analyt Technol Biomed Life Sci* 2004; 802: 329–338.
39. Lemus Gallego JM and Pérez Arroyo J. Determination of prednisolone acetate, sulfacetamide and phenylephrine in local pharmaceutical preparations by micellar electrokinetic chromatography. *J Pharm Biomed Anal* 2003; 31: 873–884.
40. Kim HS, Sun X, Lee JH, et al. Advanced drug delivery systems and artificial skin grafts for skin wound healing. *Adv Drug Deliv Rev* 2019; 146: 209–239.
41. Honeywell-Nguyen PL and Bouwstra JA. Vesicles as a tool for transdermal and dermal delivery. *Drug Discov Today Technol* 2005; 2: 67–74.
42. Ahad A, Al-Saleh AA, Al-Mohizea AM, et al. Pharmacodynamic study of eprosartan mesylate-loaded transfersomes Carbopol gel under Dermaroller® on rats with methyl prednisolone acetate-induced hypertension. *Biomed Pharmacother* 2017; 89: 177–184.
43. Woolery-Lloyd H and Kammer JN. Treatment of hyperpigmentation. *Semin Cutan Med Surg* 2011; 30: 171–175.
44. Thiyagarasaiyar K, Goh BH, Jeon YJ, et al. Algae metabolites in cosmeceutical: an overview of current applications and challenges. *Mar Drugs* 2020; 18: 323.
45. Plonka PM, Passeron T, Brenner M, et al. What are melanocytes really doing all day long. .? *Exp Dermatol* 2009; 18: 799–819.
46. Qian W, Liu W, Zhu D, et al. Natural skin-whitening compounds for the treatment of melanogenesis (Review). *Exp Ther Med* 2020; 20: 173–185.
47. Liu F, Qu L, Li H, et al. Advances in biomedical functions of natural whitening substances in the treatment of skin pigmentation diseases. *Pharmaceutics* 2022; 14(11): 12.
48. Boo YC. Arbutin as a skin depigmenting agent with anti-melanogenic and antioxidant properties. *Antioxidants* 2021; 10: 1129.
49. Liu Q, Kim C, Jo YH, et al. Synthesis and biological evaluation of resveratrol derivatives as melanogenesis inhibitors. *Molecules* 2015; 20: 16933–16945.
50. Bourhim T, Villareal MO, Gadhi C, et al. Elucidation of melanogenesis-associated signaling pathways regulated by Argan press cake in B16 melanoma cells. *Nutrients* 2021; 13: 2697.
51. Snaidr VA, Damian DL and Halliday GM. Nicotinamide for photoprotection and skin cancer chemoprevention: a review of efficacy and safety. *Exp Dermatol* 2019; 28(Suppl 1): 15–22.